3B2v7.51c GML4.3.1 JBMT : 2979 Prod.Type:COM pp.1–11(col.fig.:fig2) ED:Uma PAGN: savitha SCAN: Raghu

ARTICLE IN PRESS

Available online at www.sciencedirect.com

SCIENCE DIRECT®

Biomaterials ▮ (▮▮▮▮) ▮▮▮–▮▮▮

Biomaterials

www.elsevier.com/locate/biomaterials

Characterization of a bovine collagen–hydroxyapatite composite scaffold for bone tissue engineering

C.V.M. Rodrigues[a], P. Serricella[b], A.B.R. Linhares[c], R.M. Guerdes[d], R. Borojevic[b,c], A. Rossi[e], M.E.L. Duarte[c], M. Farina[c,*]

[a] *Programa de Engenharia Metalúrgica e de Materiais, COPPE, UFRJ, 21945-970 Rio de Janeiro, RJ, Brazil*
[b] *APABCAM, Hospital Universitário Clementino Fraga Filho, UFRJ, 21941-097 Rio de Janeiro, RJ, Brazil*
[c] *Laboratório de Biomineralização, Instituto de Ciências Biomédicas, Centro de Ciências da Saúde(CCS), Departamento de Anatomia, Universidade Federal do Rio de Janeiro (UFRJ), 21941-590 Rio de Janeiro, RJ, Brazil*
[d] *Clínica Odontológica Dr. Olympio Faissol Pinto, Rua Visconde de Ouro Preto, 63, Botafogo, Rio de Janeiro, RJ, Brazil*
[e] *Centro Brasileiro de Pesquisas Físicas CBPF/CNPq, Rua Xavier Sigaud 150, Botafogo, Rio de Janeiro, RJ, Brazil*

Received 21 October 2002

Abstract

Different biomaterials have been used as scaffolds for bone tissue engineering. Here we characterize a biomaterial composed of sintered (1100°C) and powdered hydroxyapatite (HA) and type I collagen (Coll), both of bovine origin, designed for osteoconductive and osteoinductive scaffolds. Coll/HA proportions were 1/2.6 and 1/1 (wet weight), and particles sizes varied from 200 to 400 μm. V_v (volume density) and S_v (surface to volume density) for the HA particles in the composite ranged from 0.48 ± 0.06 to 0.55 ± 0.02 and 5.090 ± 0.545 to $6.366 \pm 0.289\,\mu m^{-1}$, respectively. Due to the relatively small changes in V_v and S_v, a macroporosity could be characterized for the biocomposite. X-ray diffraction and infrared spectroscopy showed that the sintered bone was composed essentially of HA with minimum additional groups such as surface calcium hydroxide, surface and crystal water, free carbon dioxide and possibly brushite. Mass spectrometry detected carbonates at A and B sites of HA, and weakly bound to the structure. Human osteoblasts adhered and spread on both the HA particle surface and the collagen fibers, which seemed to guide cells between adjacent particles. The biocomposite studied has several characteristics considered as ideal for its use as a scaffold for osteoconduction and osteoinduction.

Keywords: Hydroxyapatite; Bovine bone; Characterization; Bone tissue engineering; Osteoblast; Collagen; Biocomposite; Biomaterial

1. Introduction

A large number of bone fractures have been treated by bone grafting, imposing wastes of the order of billions of dollars per year in United States [1]. With an increase of the mean population age, the development and optimization of bone regeneration techniques represents a major clinical need for many countries [2]. Autografts have limitations due to the necessity of an additional surgery, limited donor bone supply, anatomical and structural problems and inadequate resorption rate during healing. Allografts have the disadvantage of a potential immune response, transmitting diseases, and they may induce the loss of osteoinduction. Metals alone or coated with bioactive and bioinert ceramics have been used for load-bearing orthopedic applications, but problems due to metals corrosion, ceramics–metal interface wear, and dense fibrous tissue formation on the bone–implant interface may occur [1,3,4].

Bone tissue engineering is a new research area with clinical applications in bone replacement on orthopedic defects, bone neoplasia and tumors, pseudoarthrosis treatment, stabilization of spinal segments, as well as in maxillofacial, craniofacial, orthopedic, reconstructive, trauma and neck and head surgery [5]. It may provide solutions for generating a new bone tissue with good functional and mechanical qualities, reducing the risks and expenses of using autografts, allografts and metals. However, for improving osteoconduction and osteoin-

*Corresponding author. Fax: +55-21-562-6394.
E-mail address: mfarina@anato.ufrj.br (M. Farina).

0142-9612/03/$ - see front matter © 2003 Published by Elsevier Ltd.
doi:10.1016/S0142-9612(03)00410-1

duction, association of extracellular matrix scaffolds with osteogenic cells and growth and differentiation factors may be required [6].

During the last decades, different biomaterials of biological or synthetic origin have been designed, aiming to act as extracelular matrix scaffolds for new bone formation. Clinical uses require a series of biomaterial properties, such as bioactivity, osteoconduction, osteoinduction, biocompatibility and biodegradation; besides they should be cheap, easily produced, molded and stored [4,7–9].

Hydroxyapatite (HA), $[Ca_{10}(PO_4)_6(OH)_2]$, is one of the frequently used bioceramics for bone and dental tissues reconstitution. It has excellent biocompatibility with hard tissues [10,3], and high osteoconductivity and bioactivity despite its low degradation rate [1–4,8,11], mechanical strength and osteoinductive potential [4,11,12]. It has neither antigenicity nor cytotoxicity [4]. Collagen is biocompatible, biodegradable and osteoinductive, acting as an excellent delivery system for bone morphogenetic proteins (BMPs) [13,14]. When associated to HA particles forming a biocomposite, it prevents the HA dispersion in implants, resulting in an easily molded biomaterial [15]. Bovine collagen antigenicity may be reduced by treatments with pepsin and strong alkaline solutions, and physicochemical agents that induce cross-linking of collagen [14].

Physicochemical and crystallographic characteristics of the biomaterials will determine the osteogenic cells behavior, contributing to the success and quality of the new bone tissue. The ideal average diameter range of calcium phosphate powder particles is considered to be 200–500 μm, and particles smaller than 50 μm could induce cytotoxicity [16–19]. In calcium phosphate bioceramics, the presence of pores with average diameter in the range of 200–400 μm would support blood vessels invasion and would induce osteoblasts migration, adhesion, proliferation and differentiation inside the pores [17]. The presence of pore interconnections is an important condition for the above features to occur [20,21]. High macroporosities enhance bone formation, but values higher than 50% may lead to a loss of biomaterial's mechanical properties [21]. Microporosity and roughness determine how biological molecules and ions will be adsorbed to the biomaterial surface, affecting directly cell behavior [22]. In general, osteoblastic cells orient parallel to grooves on machined surfaces, whilst on the smooth ones they do not show any preferential organization pattern [23]. Modifications on biomaterial crystallinity and crystal sizes induced by the sintering process may also play an important role on cell adhesion, proliferation, differentiation and metabolism. Osteogenic cells seeded on synthetic HA sintered at 1100°C for 7 h presented higher proliferation, differentiation and mineralization rates than those seeded on non-sintered HA [24]. Conversely, human macrophages seeded on synthetic powders obtained from HA sintered at 900°C and 1200°C presented higher cellular activity on the former ones [25].

The interaction between cell and substrate is related to the osteogenic cells attachment, adhesion and spreading and its quality will influence cell proliferation and differentiation. The attachment phase occurs as soon as biomaterial is in contact with the cells and involves physico-chemical linkages. The adhesion and spreading phases occur when focal contacts and adhesion plaques between the substrate surface and the cell membrane are established. Osteoblast membrane receptors like integrin fix on bone extracellular matrix proteins like fibronectin, osteopontin, bone sialoprotein, thrombospondin, type I collagen and vitronectin, all containing an *Arg–Gly–Asp* (*RGD*) sequence. These proteins can be adsorbed in vitro from the serum-containing media or in vivo from biological fluids and synthesized by osteogenic cells after its adhesion on substrate surface. Actin filaments rearrangement due to adhesion process induces cell shape changes and mediates signal transduction through cytoskeleton proteins to the nuclear matrix, modifying gene expression and determining the cell capacity for proliferation and differentiation [22].

Some recent reports examined cell adhesion on calcium phosphate materials having various surface characteristics [16–19,21,23–30]; however, a few associate calcium phosphate with proteins containing RGD sequences like collagen I [15].

Some commercially available bovine calcium phosphate ceramics have been applied either in vivo or in vitro with excellent biocompatibility and osteoconduction [27,31]. Combining bovine collagen I to synthetic HA and tricalcium phosphate enhanced bone tissue formation in canine radial defects, in comparison to hydroxyapatite and tricalcium phosphate alone or associated to bone marrow aspirate [32]. It was also shown to be an effective delivery system [11]. However, there are few scientific reports related to the association of bovine collagen I to bovine HA [33].

In this work we characterized a biomaterial composed of HA powders and type I collagen, both from bovine origin, for further use as scaffolds for osteoconduction and osteoinduction. Afterwards that biomaterial was inoculated with human osteoblasts in order to evaluate its biocompatibility and cells behavior.

2. Materials and methods

2.1. Preparation of collagen/hydroxyapatite composite

Collagen/HA sample preparation was performed as previously described [33]. Briefly, type I collagen was extracted from bovine tendons, incubated in 1% sodium

hypochlorite for 24 h at 4°C followed by pepsin (1 g/kg in 10% acetic acid and 0.2% chlorhydric acid) for 24 h at 4°C. The material was centrifuged at 12,000 rpm with 10% acetic acid, subjected to "salting-out" (NaCl) and dialyzed against distilled water for 4 days, changing water daily. The collagen was stored at 4°C.

Cortical bovine bone was cleaned, soaked in 10% sodium hypochlorite for 24 h, rinsed in water and boiled in 5% sodium hydroxide for 3 h. The material was further incubated in 5% sodium hypochlorite for 6 h, washed in water and soaked in 10% hydrogen peroxide for 24 h. Samples were sintered at 1100°C (Mufla EDGCON 5P) for 3 h, pulverized (Marconi MA500) for 4 h, and grains of 200–400 μm were separated by sieving. Bone powders were sterilized at 150°C for 2 h, rinsed in tridistilled water and incubated in 1% phosphoric acid. They were rinsed again in sterile tridistilled water, and sterilized at 100°C.

The collagen-containing solution was mixed to bone powders at two different collagen/bone (HA) proportions: 1/2.6 and 1/1. A part of the collagen/HA samples was dehydrated (vacuum dessicator) and an another part was re-hydrated for 12 h with human serum, in order to mimic a possible clinical use. Samples were γ-ray irradiated with doses of 25,000 cGy. Some samples were neither dehydrated nor irradiated, and used as references for morphometric analysis.

By this way, six groups of samples subjected to different preparation methods were obtained:

(1) Dehydrated, irradiated for collagen/bone proportion of 1/2.6.
(2) Dehydrated, re-hydrated with serum and irradiated for collagen/bone proportion of 1/2.6.
(3) Non-dehydrated, irradiated for collagen/bone proportion of 1/2.6.
(4) Non-dehydrated, non-irradiated for collagen/bone proportion of 1/2.6 (reference).
(5) Non-dehydrated, irradiated for collagen/bone proportion of 1/1.
(6) Non-dehydrated, non-irradiated for collagen/bone proportion of 1/1 (reference).

2.2. Human bone cell culture

Primary human osteoblasts were obtained from the last-over material collected at surgical interventions on bones, after the agreement of the Ethical Committee of the University. The specimens (trabecular bone of femurs) were mechanically treated and washed in phosphate-buffered saline (PBS) (pH = 7.4) three times and then minced in fragments of 0.5 cm in diameter. The bone fragments were treated with collagenase IA (1 mg/ml) three times at 37°C for 1, 1.5 and 2 h, successively. The fragments were seeded into a 25 cm^2 tissue culture flask and cultured in Dulbecco's modified Eagle's medium (DMEM) and fetal bovine serum (FBS) at 37°C under the atmosphere of 95% air and 5% CO_2. After reaching confluence, the cells were trypsinized (GIBCO) and centrifuged at 1300 rpm for 5 min. The cell pellet was then resuspended in supplemented DMEM, and subcultured in a second passage at a density of 5×10^5/ml in a 25 cm^2 flask at 37°C under the atmosphere of 5% CO_2.

Alkaline phosphatase activity measurements were obtained for investigating the phenotype of the cultured osteoblast cells [15].

2.3. Cell culture on the collagen–hydroxyapatite composite

Collagen–hydroxyapatite composite with 0.5 and 0.2 cm of diameter and thickness, respectively, was placed on round glass coverslips in four-well culture plates and incubated with 1 ml of DMEM for 30 min at 37°C and under the atmosphere of 5% CO_2. The DMEM medium was discarded and 1 ml of supplemented DMEM containing osteoblast cells from the earlier passages was inoculated on the biocomposite surface and on the round glass coverslips located around the composite at a cellular density of 7×10^4 cells/ml for 4 and 11 days.

Cells seeded on round glass coverslips in the four-well culture plate without the presence of the biocomposite were used as controls.

2.4. Transmission (TEM) and scanning electron microscopy (SEM)

Bone powders were ground in an agate mortar for 10 min, suspended in 95% ethanol, and sonicated for 15 min. After allowing setting for 30 min, the supernatant was collected, dropped on formvar-covered EM grids and observed by TEM in a JEOL 1200 EX operated at 80 kV.

For SEM, part of the collagen–HA composite was fixed in 2.5% glutaraldehyde buffered at pH 7.4, dehydrated in an ethanol series and critical-point dried.

Another part of the HA–collagen composite, used for measuring volume density (V_v) and surface area to volume density (S_v) ratios [34] for HA, was fixed in the same conditions as previously described, dehydrated in acetone, embedded in epoxy resin and prepared as polished sections. Isolated bone powders (200–400 μm) were also observed by SEM in order to characterize the HA particles.

Samples inoculated with osteoblastic cells were rinsed with 0.1 M sodium cacodilate buffer (pH = 7.4), fixed for 60 min with Karnovsky's fixative (4% of paraformaldehyde and 2.5% of glutaraldehyde) in 0.1 M cacodylate buffer, pH 7.4, at room temperature and then rinsed

with the same buffer. Samples were post-fixed in 1% osmium tetroxide in 0.1 M cacodylate buffer for 20 min, dehydrated through an ethanol series, critical-point dried (Bal-Tec CPD 030) and observed by SEM.

All the samples were mounted on SEM stubs by using a double-coated carbon conductive tape (Pelco International), gold-sputtered (Balzers apparatus) and observed in a JEOL JSM-5310. *Shape factor* [(4π area)/(perimeter)^2], *Feret* diameter (diameter of a circle with the same projected area of the analyzed object), and average diameter of the isolated bone powders were measured. V_v and S_v of HA in the collagen/HA composite were obtained from the polished sections.

2.5. X-ray diffraction (XRD), Fourier transform infrared spectroscopy (FTIR) and mass spectrometry (MS)

XRD analyses of bone powders were performed on a ZEISS HZG4 high-resolution diffractometer (X-ray Source Seifert ID3000) using nickel-filtered Cu-$K_{\alpha 1}$ ($\lambda = 0.154056$ nm) radiation at a current of 4θ mA and an accelerating voltage of 40 kV. Spectra were recorded from $2\theta = 10^\circ$ to 100° at a scanning speed of 1°/min and step size of 0.02°. The HA unit-cell parameters, $a = b$ and c, were refined by using Celref software. The crystal size measured in the direction perpendicular to the diffracting planes (0 0 2) was calculated by using the Scherrer equation [35] $D = K\lambda/(\beta_{1/2}\cos\theta)$, where D is the crystal size in nanometers; K is the Scherrer constant (here $K = 1$); λ is the X-ray wavelength in nanometers; $\beta_{1/2}$ is equal to $B_{1/2} - b$, where $B_{1/2}$ is the experimental full-width at half-maximum intensity of the diffraction peak (0 0 2) and b is the width of the same peak measured on standard, perfectly crystalline HA; θ is the diffraction angle for diffraction peak (0 0 2).

The chemical composition of the amorphous and crystalline phases of the bone powder was investigated by FTIR. Samples were ground with 1% KBr in an agate mortar, compressed to tablets and analyzed under nitrogen atmosphere from 4000 to 400 cm^{-1} using a Nicolet IR 760.

MS was used to analyze the carbonate contents of the bovine HA after sintering at 1100°C. The bone powder samples were heated under helium flux from 25°C to 1200°C at 10°C/min. Thermo-programmed desorption (TPD) analysis of carbon dioxide was performed using a mass spectrometer BALZERS QUADSTAR 422 (QMS200).

2.6. Cytotoxicity analysis

Cytotoxicity of the bovine collagen/HA composite characterized was investigated by the standard "agar overlay diffusion tests" using mouse fibroblasts (C3H/AN), performed by Banco de Células do Rio de Janeiro (UFRJ, Brazil).

3. Results

3.1. Bone powder characterization

The bovine bone powder particles had irregular shapes (Fig. 1), presenting *shape factor* [(4π area)/(perimeter)^2] and *Feret diameter* values of $0.73 + 0.09$ and $254.10 + 79.31\,\mu m^{-1}$, respectively. Average diameters measured from SEM images presented an asymmetric distribution, slightly skewed towards the larger particle sizes, with the mean at $275.42 + 88.51\,\mu m$ (Fig. 2). Surface texture of the powder particles varied from rough to smooth. In rougher surfaces easily delimited grains of 0.5–10 μm (Fig. 3a) were seen, while in smoother ones the grain boundaries were poorly defined (Fig. 3b). In some cases, however, grain boundaries were observed in smooth surfaces (see Fig. 8b). Microscopic pores ranging from 0.1 to 5 μm, presenting polyhedric shapes, were observed between grains (Fig. 3b). TEM images of ground bone particles

Fig. 1. Scanning electron microscopy (SEM) image of bovine HA particles sintered at 1100°C. Particles present irregular shapes. Bar: 500 μm.

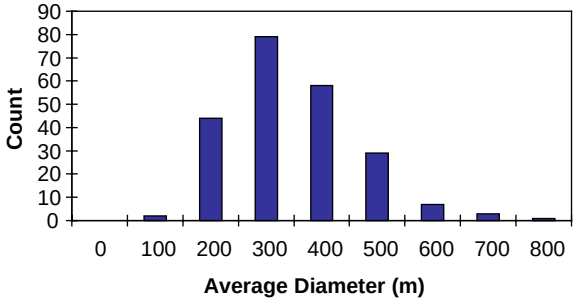

Fig. 2. Average diameter distribution for the HA particles sintered at 1100°C. Note that the distribution is slightly skewed towards the larger particle sizes.

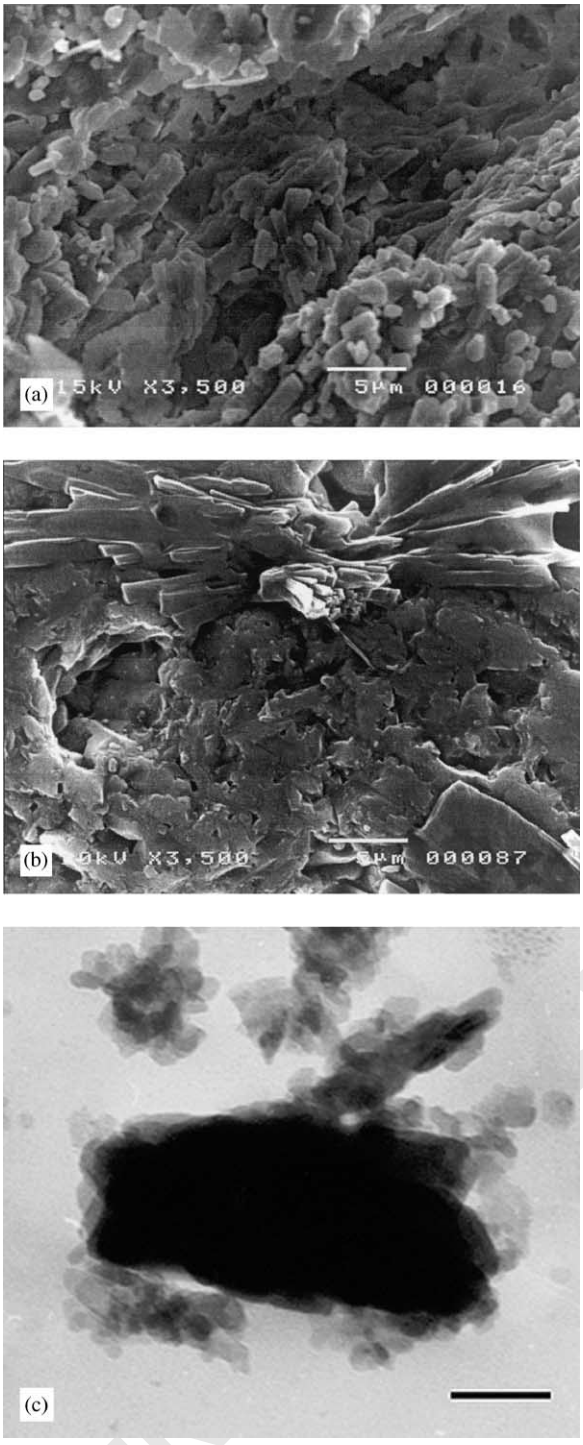

Fig. 3. Bovine bone powder particles sintered at 1100°C showing micron-sized HA grains generating different texture patterns: (a) rough surface presenting elongated HA grains; (b) smoother surface depicting polyhedric microscopic pores; bar for (a) and (b): 5 µm. (c) Transmission electron microscopy image of ground bone powder particles showing individual crystallites of HA; bar: 85 nm.

showed single crystals in the nanometer range (Fig. 3c). Plate-shaped-like crystals possibly composed of brushite (see Fig. 6 for FTIR data) were rarely observed inside the Havers channels (Fig. 4).

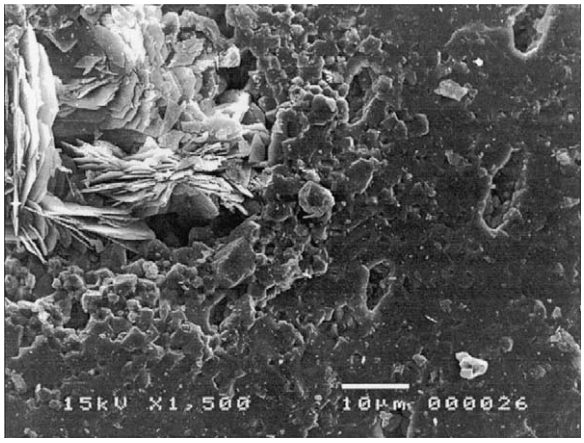

Fig. 4. Plate-shaped-like crystals inside Havers channels on HA grains subjected to 1% phosphoric acid incubation; bar: 10 µm.

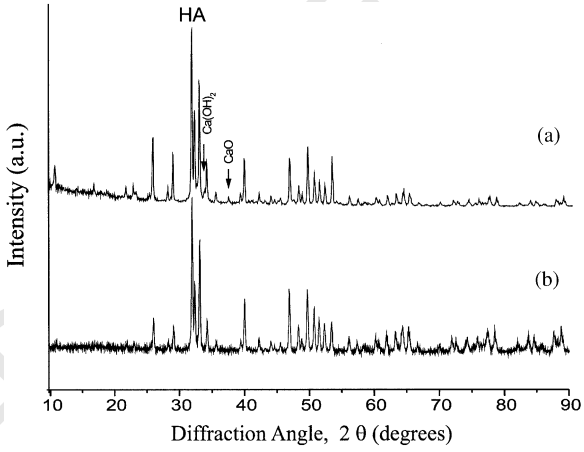

Fig. 5. X-ray diffraction (XRD) spectra of bovine bone powder: (a) non-subjected and (b) subjected to incubation in 1% phosphoric acid. Both samples are highly crystalline and composed of HA. Note the presence of detectable peaks of CaO and $Ca(OH)_2$ in (a).

XRD patterns of the bone powders showed that the material is highly crystalline and composed of HA crystals (JCPDS card No. 9-432) (Fig. 5b). CaO and $Ca(OH)_2$ were detected by XRD analyses only for samples not subjected to incubation in 1% phosphoric acid (Fig. 5a). The average crystal dimension in the direction perpendicular to the diffracting planes (0 0 2) (D_{002}) was 58.4 nm. The refined unit-cell parameters of HA showed *a*-, *b*- and *c*-axis values ($a = b = 0.94299$ nm and $c = 0.68909$ nm).

FTIR spectra of the analyzed bone powder samples revealed typical bands of HA (3570, 3535, 3430, 2140–1980, 1090, 1044, 957, 629, 601 and 570 cm^{-1}) with carbonates occupying A (1550, 1500, 1462 and 877 cm^{-1}) and B (1455, 1411 and 872 cm^{-1}) sites (Fig. 6B) [31,36,37]. Minor phases corresponding possibly to the presence of crystal water and surface adsorbed water (3430 and 1620 cm^{-1}), calcium hydroxide (3640 cm^{-1}), brushite (1219 and 874 cm^{-1}) [32] and free carbon dioxide (2350 cm^{-1}) [37] were also present in the

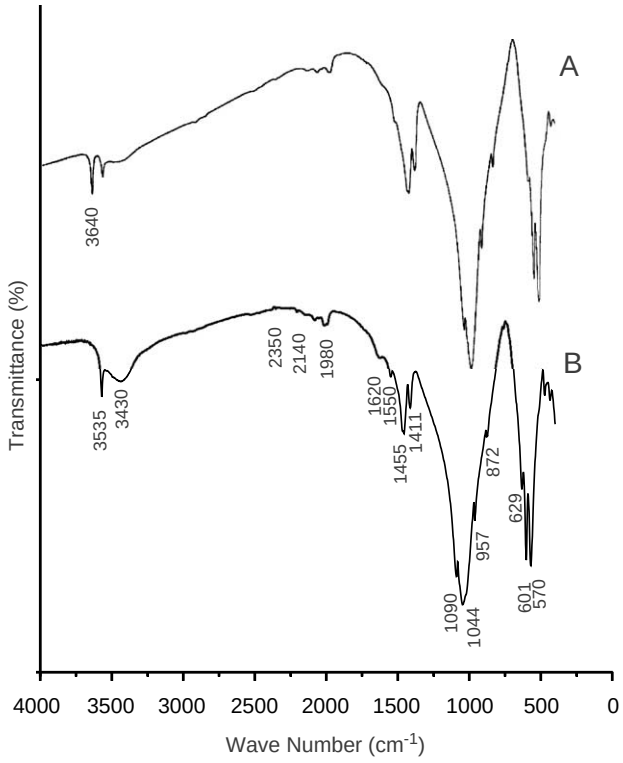

Fig. 6. Infrared spectra obtained from the samples of bovine bone sintered at 1100°C: (A) non-subjected and (B) subjected to the treatment with 1% phosphoric acid. Bands of HA (3570, 3535, 3430, 2140–1980, 1090, 1044, 957, 629, 601 and 570 cm^{-1}) with carbonates occupying A (1550, 1500, 1462 and 877 cm^{-1}) and B (1455, 1411 and 872 cm^{-1}) sites are seen. Minor phases corresponding possibly to crystal water and surface adsorbed water (3430 and 1620 cm^{-1}), calcium hydroxide (3640 cm^{-1}), brushite (1219 and 874 cm^{-1}) and free carbon dioxide (2350 cm^{-1}) were also detected. Note that band at 3640 cm^{-1} is much larger in (A) than in (B).

samples. Samples not subjected to incubation in 1% phosphoric acid presented FTIR spectra very similar to the ones subjected to that treatment, unless for the intense band at 3640 cm^{-1}, probably due to calcium hydroxide (Fig. 6A) [31].

TPD analyses of carbon dioxide using MS for all the samples studied indicated a strong loss of CO_2 for temperatures around 670°C and a weak desorption at 1020°C (Fig. 7). This loss of carbon dioxide can be attributed to the existence of carbonate groups occupying mostly B (phosphate sites) and A (hydroxyl sites) sites, respectively, both at the HA surface and in the bulk structure.

3.2. Collagen morphologic characterization

In general, collagen in the collagen–HA composite samples had a fibrillar aspect (Fig. 8a). It was disposed as locally oriented long fibers or irregular networks adhered to bone powder particles surface. Dehydrated samples presented collagen mainly as oriented fibers punctually adhered to bone particles surface (Fig. 8b),

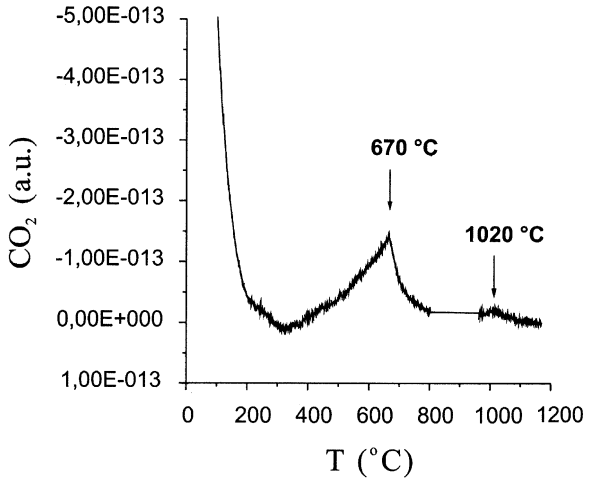

Fig. 7. Thermo programmed desorption (TPD) analysis of carbon dioxide using mass spectrometry (MS) for bovine bone powder sintered at 1100°C. Weakly bound and B type carbonates (670°C) are present in higher amounts than the carbonates at A sites (1020°C).

while re-hydrated samples chiefly as irregular compact networks widely adhered to HA surface (Fig. 8c). The irradiation of the samples at the level used (25,000 cGy) did not induce major changes in the collagen morphology.

3.3. Morphometric analysis

Volume density of HA particles, V_v, ranged from $0.48+0.06$ to $0.55+0.02$; however, V_v values for group VI samples (reference sample, collagen/bone proportion of 1/1) were significantly higher than for other groups analyzed (Student, $p<0.05$). Samples of the groups I–V had data that were not significantly different (ANOVA, $p<0.05$) (Table 1).

Surface area to volume density of HA particles, S_v, of the samples studied ranged from $5.09+0.55$ to $6.37+0.29\,\mu m^{-1}$. However, S_v values for groups V and VI samples (proportion collagen/bone of 1/1) were significantly higher than for other groups analyzed (Student, $p<0.05$). Samples of the groups I–IV have data not significantly different (ANOVA, $p<0.05$) (Table 1).

3.4. Cytoxicity evaluation and osteoblast–composite interaction

No cellular degeneration or death was observed in the standard cytotoxicity assays of the biomaterial samples studied.

Osteoblast cells cultured for 4 days on the composite surface were rare (possibly due to the number of cells used and the high total surface area of the HA particles) (not shown).

At 11 days after seeding, cells exhibited a high degree of proliferation and partially covered the composite

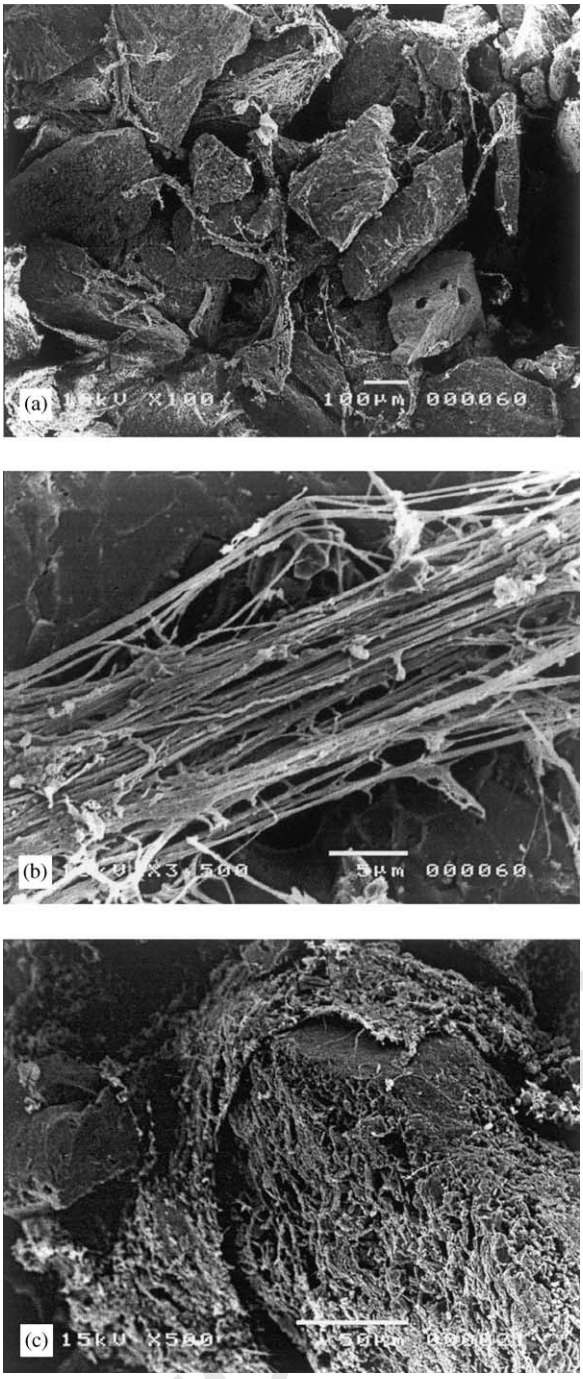

Fig. 8. SEM images of collagen–HA biocomposite. (a) Non-dehydrated, non-irradiated sample corresponding to a collagen/bone proportion of 1/1. Collagen is organized as fibers both attached to the particle's surfaces or linking different particles; bar: 100 µm. (b) Detail of a sample similar to the previous one showing a bundle of aligned collagen fibers over a smooth area of HA. Grain contours are seen in the HA surface; bar: 5 µm. (c) Dehydrated, re-hydrated and irradiated sample corresponding to a collagen/bone proportion of 1/2.6. In this case collagen forms a compact mesh widely adhered to HA surface; bar: 50 µm.

surface (Fig. 9). They migrated through the composite block reaching its bottom surface and then the coverslip and also from the coverslip to the composite surface. At that time, osteoblasts presented polygonal shape and were strongly attached to the surface of the bone particles (Fig. 10) and also to the collagen fibers (Figs. 11a and b).

Table 1
Morphometric data (mean ± standard deviation) of the volume density (V_v) and the surface to volume density (S_v) of HA powder particles

Group	V_v	S_v (μm^{-1})	N
I	0.49 ± 0.04	5.610 ± 0.548	11
II	0.48 ± 0.06	5.090 ± 0.545	10
III	0.51 ± 0.04	5.412 ± 0.392	11
IV	0.50 ± 0.03	5.579 ± 0.381	06
V	0.52 ± 0.03	6.366 ± 0.289	06
VI	0.55 ± 0.02	6.019 ± 0.555	06

(I) Dehydrated, irradiated for collagen/bone proportion of 1/2.6; (II) Dehydrated, re-hydrated with serum and irradiated for collagen/bone proportion of 1/2.6; (III) Non-dehydrated, irradiated for collagen/bone proportion of 1/2.6; (IV) Non-dehydrated, non-irradiated for collagen/bone proportion of 1/2.6 (reference); (V) Non-dehydrated, irradiated for collagen/bone proportion of 1/1; (VI) Non-dehydrated, non-irradiated for collagen/bone proportion of 1/1 (reference).

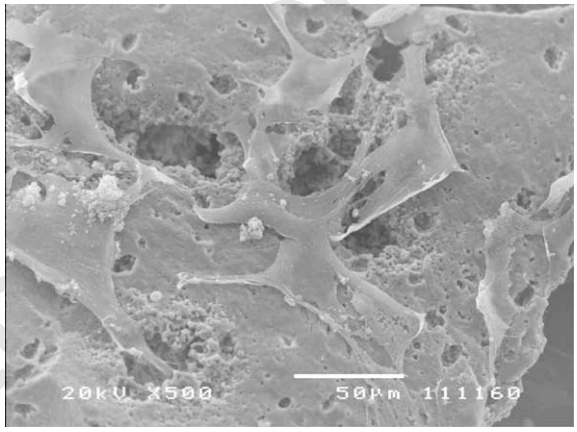

Fig. 9. Polygonal osteoblasts partially covering the composite surface, 11 days after seeding; bar: 50 µm.

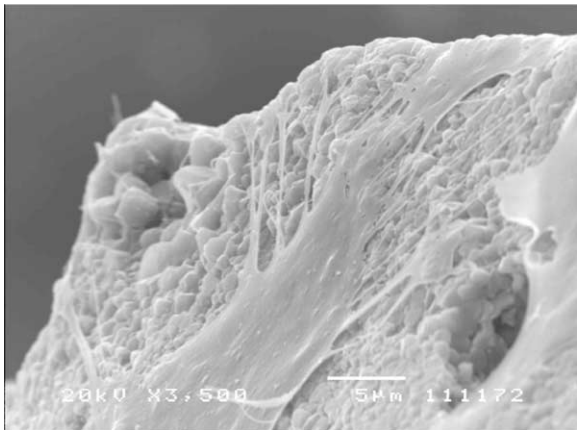

Fig. 10. Osteoblasts exhibiting cytoplasmatic projections strongly attached to HA surface, 11 days after seeding; bar: 5 µm.

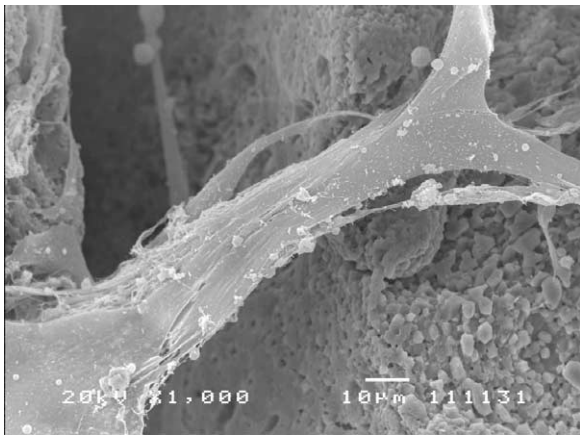

(a)

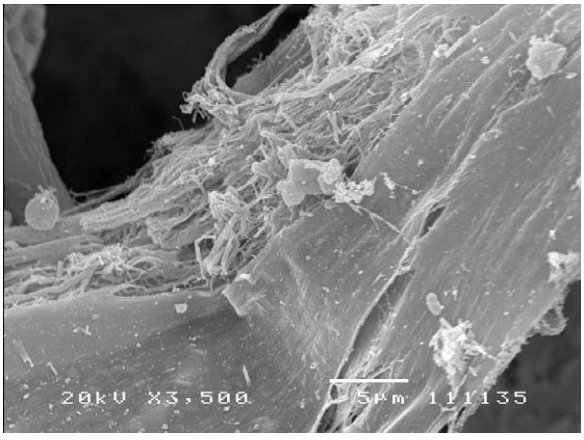

(b)

Fig. 11. Osteoblasts attached to collagen fibers (a) connecting two adjacent bone particles (bar: 10 µm) and (b) details (bar: 5 µm) 11 days after seeding.

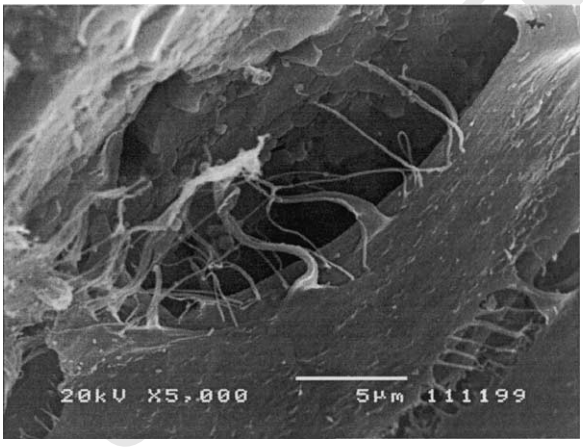

Fig. 12. Osteoblasts attached preferentially to HA micropores 11 days after seeding; bar: 5 µm.

In some regions osteoblastic cells were preferentially adhered to HA micropores (Fig. 12). Cell distribution along the bulk of the composite seemed to follow the same distribution of the collagen fibers, when compared to control images (composite without cells). Some cells were attached to two separate HA particles by following collagen fibers (See Fig. 11a).

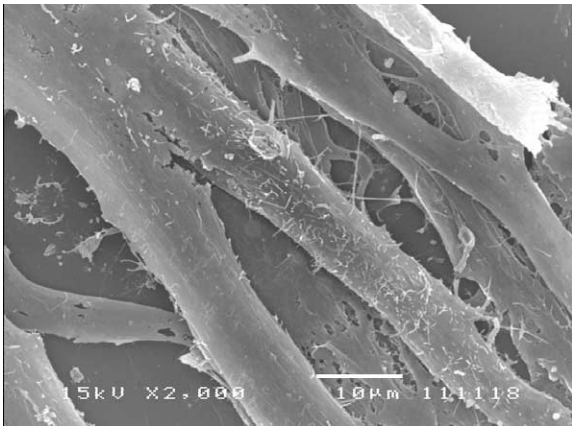

Fig. 13. Reference sample showing osteoblasts in a post-confluent pattern 11 days after seeding; bar: 10 µm.

Reference sample showed high osteoblast proliferation and adhesion rate and a post-confluent pattern 4 days after seeding (Fig. 13).

4. Discussion

XRD and FTIR analyses showed that bone powders were composed essentially of HA with additional carbonate groups distributed at A and B sites. Small amounts of calcium hydroxide, surface adsorbing and crystal water, free carbon dioxide and possibly brushite were detected by FTIR. Bone powders had a mean particle size of $275.42 + 88.51$ µm, which has been considered ideal for osteogenesis [16,17,38].

Despite possible morphological changes due to critical-point drying of the samples prior to SEM analyses, the observed alterations on collagen morphology and attachment to HA surface seemed to be directly related to dehydration and re-hydration procedures. The dehydration procedure resulted mainly in locally oriented collagen fibers punctually adhered to bone particles surface, while re-hydration procedure formed irregular networks of collagen fibrils widely adhered to HA surface.

Table 1 shows that, although V_v values from group VI samples and S_v values from groups V and VI were significantly different from the other groups, the absolute value of these differences were very small. As a consequence, we can conclude from the morphometric analysis that increasing the collagen content (collagen/HA ratio) did not affect in great extent V_v and S_v. It means that the total contact area per unit volume available for osteogenic cells to attach directly onto HA surface does not vary in great extent when more collagen

is present in the sample. However, it is expected that the total contact area of collagen available to cells to adhere increases as a function of the collagen content. The values of V_v found indicate that almost half of the biomaterial volume corresponds to the mineral phase and the other part to collagen plus "void". The presence of collagen linking contiguous bone particles makes it possible to define a macroporosity for the biocomposite. Considering that collagen is disposed in plates or fibers (with minimum volume) and that osteoblastic cells are capable of secreting collagenase, remodeling the collagen molecules, the total macroporosity may be considered as corresponding to the volume percentage occupied by collagen plus "void", i.e. about 50% (Table 1). This value is similar to the ideal one proposed previously [21]. An additional advantage of this biocomposite is that it is moldable with possibly minimum changes in V_v and S_v.

The sintering process of bovine HA caused an increase in the sample crystallite size and induced HA densification resulting in grains growth with the formation of dense grain boundary phases and polyhedric submicron-sized pores [39]. As previously reported for synthetic samples, crystal and grain growth is associated with crystallinity and density increase, and with decrease of the total porosity and the sample surface area [40]. In accordance with the above-described changes in sintered HA, we observed that individual grains were larger in the 1100°C sintered HA than for temperatures of 600°C and 900°C (not shown). Also polyhedric-shaped microscopic pores were observed in 1100°C sample (Fig. 3b).

The detection of CaO and $Ca(OH)_2$ by XRD of the bovine bone studied in this work can be attributed to the decomposition of a HA with a Ca/P ratio higher than 1.67 (typical of bovine bone HA) caused by the high sintering temperature [31]. Moreover, CaO reacts with water molecules [3] giving $Ca(OH)_2$, which was detected by FTIR. CaO and $Ca(OH)_2$ on the bone powders surface studied was decreased by 1% phosphoric acid incubation.

MS results showed that samples presented structural carbonates distributed at A and B sites of HA. Carbonates weakly bound to HA structure could also be present. These were probably distributed on crystal surface and in crystal lattice vacancies. Those vacancies resulted from ions displacement due to loss of carbonates and OH groups during sintering process. Vacancies could also be present due to entering of carbonates inside B and A sites of HA, along the formation of natural bone mineral phase.

During the cooling process inside the furnace, the carbon dioxide formed could have occupied vacancies present on natural bovine bone or could have been disposed on its surface, weakly bound. The presence of weakly bound carbonates on the HA lattice structure would be important in the formation of a carbonate–HA layer after dissolution and re-precipitation of mineral phases in the surface of the biomaterial. Some authors consider that this layer is very important in the cell adhesion process [1].

Phosphoric acid (1%) incubation of bone powders was probably responsible for the precipitation of minimal amounts of other phosphates as brushite plaque-like crystals (SEM and FTIR) with low solubility in water on HA surface [41].

Human osteoblast cells inoculated on composite surface were sparse after 4 days of seeding with the concentration used (7×10^4 cells/ml). Polygonal cells were seen after 11 days when the cells proliferation, adhesion and spreading were more intense. The adhesion did not occur preferentially to HA crystals or to collagen fibrils and its quality seemed not dependent on the texture or roughness of the biomaterial surface as reported by some authors [17,22–23,26]. Some contact points of cells on HA were preferentially located on HA micropores (Fig. 12).

It was reported that the bioactivity and ability to form a strong interface bone–biomaterial is related to the formation of carbonated HA on the bioactive glasses and calcium phosphate biomaterials surface, in vitro and in vivo. In this way, there are organic and inorganic processes related to the interaction between substrate surface and serum, biologic fluids and/or cells causing the dissolution of surface material and precipitation of micron-sized crystals of carbonated HA [8]. The formation of a carbonated HA crystals layer associated to the adsorption and incorporation of biological molecules and ions on the substrate surface would mediate effects on the cells activity, including adhesion, proliferation and differentiation [1]. However, the selective adsorption of proteins present in the serum, as fibronectin and vitronectin, may also have had an important role on osteoblasts adhesion [26]. After the beginning of the adhesion process serum proteins associated to those secreted from osteoblastic cells attached to substrate surface may have contributed to enhance the adhesion process [22].

The collagen-binding molecules such as fibronectin, which may be readily supplied from plasma, contain RGD sequences that mediate interaction with cell membrane integrins and promote cell attachment through focal contacts and adhesion plaques [9]. The utilization of bovine collagen organized as three-dimensional arrays in contact with bone powder particles enhances the contact guidance process of human osteoblasts inoculated onto the biocomposite surface [42].

Biological tests for evaluating biomaterial cytoxicity indicated that the HA–collagen composite were non-toxic to testing cells.

5. Conclusions

The success of applying biomaterials composed of collagen and HA as scaffolds for generating a new bone tissue is related to the fact that this combination is biocompatible and forms a favorable three-dimensional matrix for human osteoblast cells to adhere and spread, associating the advantage of collagen osteoinduction to the superior bioactivity and osteoconduction of HA [11,15,43]. Collagen also enhances the adhesion and contact guidance process of osteoblasts inoculated to the collagen–HA composite surface [42] through specific Arg–Gly–Asp (RGD) sequences that mediate the adhesion interaction between integrins and substrate surface [9].

The biomaterial analyzed and characterized here had some properties and characteristics reported by the literature as ideal for enhancing the generation of a new bone tissue. Among these characteristics we include the diameter of particles, presence of collagen, optimal macroporosity caused by collagen–particles interaction, presence of weakly bound carbonate groups into the HA (at site B) that can potentially generate carbonate–HA on particles surface considered to be very important in cells adhesion and further cellular behavior.

Acknowledgements

We acknowledge the Brazilian Programs/Institutions: Instituto do Milênio de Bioengenharia Tecidual/CNPq; Centro Brasileiro de Pesquisas Físicas; Instituto de Biofísica Carlos Chagas Filho/UFRJ; Laboratório de Instrumentação Nuclear/UFRJ.

References

[1] Ducheyne P, Qiu Q. Bioactive ceramics: the effect of surface reactivity on bone formation and bone cell function. Biomaterials 1999;20:2287–303.
[2] Green D, Walsh D, Mann S, Oreffo ROC. The potential of biomimesis in bone tissue engineering: lessons from the design and synthesis of invertebrate skeletons. Bone 2002;30(6):810–5.
[3] Suchanek W, Yoshimura M. Processing and properties of hydroxyapatite-based biomaterials for use as hard tissue replacement implants. J Mater Res 1998;13(1):94–117.
[4] Burg KJL, Porter S, Kellam JF. Biomaterial developments for bone tissue engineering. Biomaterials 2000;21:2347–59.
[5] Lawson AC, Czernuszka JT. Collagen–calcium phosphate composites. Proc Instr Mech Eng 1998;212(11):413–25.
[6] Bruder SP, Fox BS. Tissue engineering of bone. Clin Orthop Rel Res 1999;367S:S68–83.
[7] Pilliar RM, Filiaggi MJ, Wells JD, Grynpas MD, Kandel RA. Porous calcium polyphosphate scaffolds for bone substitute applications—in vitro characterization. Biomaterials 2001;22:963–72.
[8] LeGeros RZ, LeGeros JP, Daculsi G, Kijkowska R. Calcium phosphate biomaterials: preparation, properties and biodegradation. In: Wise DL, Trantolo DJ, Altobelli DE, Yaszemski MJ, Gresser JD, Schwartz ER, editors. Encyclopedic handbook of biomaterials and bioengineering, Part A: materials, vol. II. New York, USA: Marcel Dekker; 1995. p. 1429–63.
[9] Boyan BD, Lohmann CH, Romero J. Bone and cartilage tissue engineering. Clin Plast Surg 1999;26(4):629–45.
[10] Wozney JM, Rosen V. Bone morphogenetic protein and bone morphogenetic protein gene family in bone formation and repair. Clin Orthop Rel Res 1998;346:26–37.
[11] Asashina I, Watanabe M, Sakurai N, Mori M, Enomoto S. Repair of bone defect in primate mandibule using a bone morphogenetic protein (BMP)–hydroxyapatite–collagen composite. J Med Dent Sci 1997;44:63–70.
[12] Reddi AH. Morphogenesis and tissue engineering of bone and cartilage: inductive signals, stem cells, and biomimetic materials. Tissue Eng 2000;6(4):351–9.
[13] Reddi AH. Role of morphogenetic proteins in skeletal tissue engineering and regeneration. Nat Biotechnol 1998;16:247–52.
[14] Chevallay B, Herbage D. Collagen-based biomaterials as 3D scaffold for cell cultures: applications for tissue engineering and gene therapy. Med Biol Eng Comput 2000;38:211–8.
[15] Hsu FY, Chueh SC, Wang YJ. Microspheres of hydroxypapatite/reconstituted collagen as supports for osteoblast cell growth. Biomaterials 1999;20:1931–6.
[16] Evans EJ. Toxicity of HA in vitro: the effect of particle size. Biomaterials 1991;12:574–6.
[17] Boyan BD, Hummert TW, Dean DD, Schwartz Z. Role of material surfaces in regulating bone and cartilage cell response. Biomaterials 1996;17(2):137–46.
[18] Higashi T, Okamoto H. Influence of particle size of hydroxyapatite as a capping agent on cell proliferation of cultured fibroblasts. J Endodontics 1996;22(5):236–9.
[19] Sun J-S, Tsuang Y-H, Chang WH-S, Li J, Liu H-C, Lin F-H. Effect of hydroxyapatite particle size on myoblasts and fibroblasts. Biomaterials 1996;18:683–90.
[20] Tsuruga E, Takita H, Itoh H, Wakisaka Y, Kuboki Y. Pore size of porous hydroxyapatite as the cell-substratum controls BMP-induced osteogenesis. J Biochem 1997;121:317–24.
[21] Lu JX, Flautre B, Aselme K, Hardouin P, Gallur A, Descamps B, Thierry B. Role of interconnections in porous bioceramics on bone recolonization in vitro and in vivo. J Mat Sci: Mater Med 1999;10:111–20.
[22] Anselme K. Osteoblast adhesion on biomaterials. Biomaterials 2000;21:667–81.
[23] Anselme K, Bigerelle M, Dufresne E, Judas D, Hardouin P. Qualitative and quantitative study of human osteoblast adhesion on materials with various surface roughness. J Biomed Mater Res 2000;49(2):155–66.
[24] Villareal DR, Sogal A, Ong JL. Protein adsorption and osteoblast responses to different calcium phosphate surfaces. J Oral Implantol 1998;21(2):67–73.
[25] Harada Y, Wang J-T, Doppalapudi VA, Willis AA, Jasty M, Harris W, Nagase M, Goldring SR. Differential effects of different forms of hydroxyapatite and hydroxyapatite tricalcium phosphate particulates on human monocyte macrophages in vitro. J Biomed Mater Res 1996;31:19–26.
[26] Deligianni DD, Katsala ND, Koutsoukos PG, Missirlis YF. Effect of surface roughness of hydroxyapatite on human bone marrow cell adhesion, proliferation, differentiation and detachment strength. Biomaterials 2001;22:87–96.
[27] Açil Y, Terheyden H, Dunsche A, Fleiner B, Jepsen S. Three-dimensional cultivation of human osteoblast-like cells on highly porous natural bone mineral. J Biomed Mater Res 2000;51:703–10.

[28] Matlaga BF, Yasenchak LP, Salthouse TN. Tissue response to implanted polymers: the significance of sample shape. J Biomed Mater Res 1976;10:391–7.

[29] Misiek DJ, Kent JN, Carr RF. Soft tissue responses to hydroxyapatite particles of differente shapes. J Oral Maxillofac Surg 1984;42:150–60.

[30] Grégoire M, Orly I, Menanteau J. The influence of calcium phosphate biomaterials on human bone cell activities. An in vitro approach. J Biomed Mater Res 1990;24:165–77.

[31] Joschek S, Nies B, Krotz R, Gopferich A. Chemical and physicochemical characterization of porous hydroxyapatite ceramics made of natural bone. Biomaterials 2000;21:1645–58.

[32] Johnson KD, Frierson KE, Keller TS, Cook C, Scheinberg R, Zerwekh J, Meyers L, Sciadini MF. Porous ceramic as bone graft substitutes in long bone defects: a biomechanical, histological, and radiographic analysis. J Orthop Res 1996;14:351–69.

[33] Vidal BC. The use of a complex of collagen type I with hydroxyapatite from bone, as a bone implant substitute: an experimental approach. Tissue Eng 1996;2(2):151–60.

[34] Underwood EE. Quantitative stereology. Reading, MA: Addison-Wesley Publishing Company; 1970. p. 274.

[35] Radin SR, Ducheyne P. The effect of calcium phosphate ceramic composition and structure on in vitro behavior. II. Precipitation. J Biomed Mater Res 1993;27:35–45.

[36] Ou-Yang H, Paschalis EP, Mayo WE, Boskey AL, Mendelsohn R. Infrared microscopic imaging of bone: spatial distribution of CO_3^{-2}. J Bone Min Res 2001;16(5):893–900.

[37] Vignoles M, Bonel G, Holcomb DW, Young RA. Influence of preparation conditions on the composition of type B carbonated hydroxyapatite and on the localization of the carbonate ions. Calcif Tissue Int 1988;43:33–40.

[38] Shapoff CA, Bowers GM, Levy B, Mellonig JT, Yukna RA. The effect of particle size on the osteogenic activity of composite grafts of allogeneic freeze-dried bone and autogenous marrow. J Periondotol 1980;51(11):625–30.

[39] Petrov OE, Dyulgerova E, Petrov L, Popova R. Characterization of calcium phosphate phases obtained during the preparation of sintered biphase Ca–P ceramics. Mater Lett 2001;48:162–7.

[40] Muralithran G, Ramesh S. The effects of sintering temperature on the properties of hydroxyapatite. Ceram Int 2000;26:221–30.

[41] Chow IC, Brown WE. Phosphoric acid conditioning of teeth for pit and fissure sealants. J Dent Res 1973;52(5):1158.

[42] Dunn GA, Ebendal T. Contact guidance on oriented collagen gels. Exp Cell Res 1978;111:475–9.

[43] Lawson AC, Czernuszka JT. Collagen–calcium phosphate composites. Proc Instr Mech Eng 1998;212(11):413–25.